Egypt.J.Chem. **Vol. 62**, No. 8. pp. 1519 - 1536 (2019)

Egyptian Journal of Chemistry
http://ejchem.journals.ekb.eg/

Spectroscopic Investigation of Para-Methyl and Para-Methoxy Maleanilinic Acids in Comparison with Thermal Analyses and Theoretical Calculations and Evaluation of Cytotoxicity against Carcinoma Cells

Mohamed A. Zayed[*1], Mohamed El-desawy[2], Azza A. Eladly[3]
[1]*Chemistry Department, Faculty of Science, Cairo University, Giza-12613, Egypt.*
[2]*Nuclear Physics Department, Nuclear Research Center, AEA, 13759-Cairo, Egypt.*
[3]*Science and Technology Center of Excellence, Military production, M P P, P.O. Box 3066, Elsalam II, Cairo, Egypt.*

TWO NOVEL N-maleanilinic acid derivatives (I-II) namely (E) – oxo -4- ((4- methyl phenyl) amino)-4- oxobut-2-enoic acid (p-MMA) and (E) -4- ((4- methoxy phenyl) amino)-4- oxobut -2- enoic acid (p-MOMA) were prepared by solvent free reaction between maleic anhydride, p- methyl and p-methoxy aniline derivatives in a good yield. These compounds were synthesized and investigated using elemental analyses, FT-IR and thermal analyses under argon atmosphere. The crystallographic structures of studied compounds were investigated by X-ray diffraction (XRD). The molecular structures of the titled compounds in the ground state were optimized by DFT/B3LYP and HF methods with 6-311G++ (d,p) basis set. Calculations were carried out by GAUSSIAN 09 suite of programs. Natural bond orbitals (NBO) analysis and frontier molecular orbitals were performed using NBO 3.1 program implemented in the Gaussian 09 package are presented at the same level of theory. These results were tabulated. This research aims chiefly to correlate between the structures of these investigated derivatives using experimental techniques in comparison with the theoretical molecular orbital (MO) calculated parameters. This correlation between experimental and theoretical calculations provided a good confirmation of the proposed structures of the newly prepared compounds. The derivatives were found to be highly effective against Hepatocellular carcinoma cells > Breast carcinoma cells > colon carcinoma cells. It was recognized, that cancer cells over expression promotes tumorigenic functions; were suppressed by p-MMA > p-MOMA inhibitors.

Keywords: N-maleanilinic acids, spectroscopy (FT-IR), Thermal analyses, XRD, DFT calculations, Biological activity against Carcinoma cells.

Introduction

The aim of this research the synthesis and investigation of two novel maleanilinic acids derivatives in different solvents were performed [1-6]. N-substituted maleanilinic acid derivatives can be used to prepare the maleimides: which are an important class of substrates for biology as chemical probes of protein structure [7]. It can be used as protective and curative fungicides [8]. In polymer chemistry they can be used as photo initiators for free-radical polymerization [9,10]. They can also be used as monomers in poly-maleimides or their copolymers synthesis. The computational chemistry [11] is rapidly growing; using home computers and getting faster; which can be used for the interpretation of experimental results [12]. Therefore, this paper is mainly focused on studying molecular structure reactivity

*Corresponding author e-mail: mazayed429@yahoo.com, Tel: 002-01005776675
Received 17/1/2019; Accepted 7/3/2019
DOI: 10.21608/EJCHEM.2019.7353.1597

relationship of maleanilinic acid derivatives via investigation of their decomposition mechanisms using thermal (TA) in comparison with the theoretical molecular orbital calculations. They can also be used as monomers in poly-maleimides or their copolymers synthesis. The experimental results obtained are also correlated with the theoretical data of MOCS to identify the weakest bonds broken during both mass and thermal studies. Knowing this structural session of bonds can be used to decide the active sites of these derivatives responsible for their chemical and biological properties. These derivatives are tested against cancer cells as health applications to confirm their life importance.

Experimental

Materials and Methods

Analytes

All chemicals used were purchased from Arcos, Oxford and Merck Chemical Co. (Germany). Maleic anhydride, P-Toluidine, 99% crystalline and P-Methoxy aniline were used as received. Two N-maleanilinic acids were prepared according to the procedures reported in the literature [13]. Aniline derivative of 12.75 g (0. 1 mol) was mixed and ground at room temperature with maleic anhydride 9.8 g (0. 1 mol) in an agate mortar. During crunching processes greenish-yellow color products appeared. The grinding was continued for 30 min or more. The crude products were crystallized from ethanol and the collected greenish-yellow crystals were dried. Analytical parameters of the prepared N-substituted maleanilic acids are listed in Table 1.

Instruments

Elemental microanalysis of the synthetized compounds and separated solids, for C, H and N were performed in the Microanalytical Centre, Cairo University using Elementar CHNS analyzer, model Vario EL III.

Thermal analyses (TA) of two N-Maleanilic acid derivatives (I-II) were measured using thermal analyzer of TA Q500. The mass losses of p-MMA and p-MOMA 1.71, 3.42 mg samples respectively and the changes of the samples with temperature were measured from room temperature up to 500^{o} C. The heating rates in an argon atmosphere were 5, 10 and 15 ^{0}C min^{-1}. These instruments were calibrated using indium metal as a thermally stable material.

The FT-IR spectra were recorded on Thermo Electron Corporation, Madison, WI 53711, USA in range of 4000-400 cm^{-1}. The spectral resolution is ± 2 cm^{-1} using KBr disc technique.

The molecular structures of Maleanilinic acid derivatives (I-II) in the ground states were optimized (Fig. 1) by a DFT method and using B3LYP functional [14,15] combined with 6-311G++(d,p) basis set [16]. In this work, the calculations have been carried out on p-MMA and p-MOMA molecules; neutral molecule (related to TA decomposition) and charged molecular ion (related to MS fragmentation); which have been then used for prediction of the weakest bond broken to follow the fragmentation pathways in both techniques. The calculations were carried out using GAUSSIAN 09 [17] suite of programs. Natural bond orbitals (NBO) analysis and frontier molecular orbitals were performed using NBO 3.1 program [18] implemented in the GAUSSIAN 09 package at the DFT/B3LYP/6-311G++(d,p) at the same level.

The crystallite phases of different samples

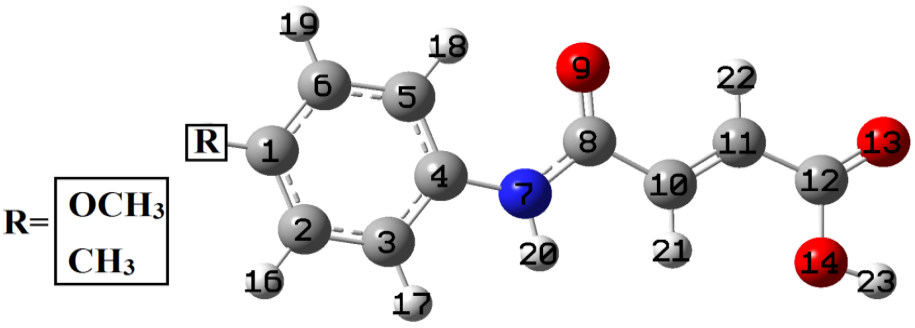

Fig. 1. The optimized structures of derivatives-maleanilinic acid with their numbering system.

were identified by Powdered X-ray diffraction (XRD) using a step size of 0.04◦ and at a scanning rate of 1.2◦/min with continuous Scan mode on a ARL™ X'TRA Powder diffractometer, Thermo Fisher Scientific Inc. Available at Science and technology of excellence (STCE) with crystallographic data software Winxrd program attached with ICDD laboratory information using metal ceramic tube Copper Target (with Cu-K-alpha wave length=1.5405981 A°) radiation operating at accelerating voltage and applied current were 44 kV and 45 mA, respectively, Ni Filter and scintillation detector (NaI (TI) scintillation crystal). The diffraction data was recorded for 2Θ values between 10◦ and 70◦.

Cytotoxicity studies and procedures

Cytotoxicity studies and procedures were involved the following [19,20]:

Mammalian cell lines: MCF-7 cells (human breast cancer cell line), HepG-2 cells (human Hepatocellular carcinoma) and HCT-116 (colon carcinoma) were obtained from VACSERA Tissue Culture Unit.

Chemicals Used: Dimethyl sulfoxide (DMSO), crystal violet and trypan blue dyes were purchase from Sigma St. Louis, Mo., USA. Fetal Bovine serum, DMEM, RPMI-1640, HEPES buffer solution, L-glutamine, gentamycin and 0.25% Trypsin-EDTA were purchased from Lonza.

Crystal violet stain (1%): It composed of 0.5g of crystal violet with 50 mL methanol; which dissolved then made up to volume 100 mL with double distilled H_2O and filtered through a Whatmann No.1 filter paper.

Cell line Propagation: The cells were propagated in Dulbecco's modified Eagle's medium (DMEM) supplemented with 10% heat-inactivated fetal bovine serum, 1% L-glutamine, HEPES buffer and 50µg/mL gentamycin. All cells were maintained at 37ºC in a humidified atmosphere with 5% CO_2 and were subcultured two times a week.

Results and Discussion

Structural determination of N-Substituted maleanilic acids

Two n-substituted Maleanilinic acid derivatives (I-II) were prepared by reaction between solid maleic anhydride (MA) and various solid N-substituted anilines at room temperature by solvent-less procedure. The prepared Maleanilinic acids are depicted in Scheme 1. The synthetic method used to prepare novel maleanilinic acid derivatives is simple, clean, economic and nearly quantitative of high yields (Table 1).

The elemental analyses of the prepared compounds and their analytical parameters are given in Table 1.

The vibrational spectra

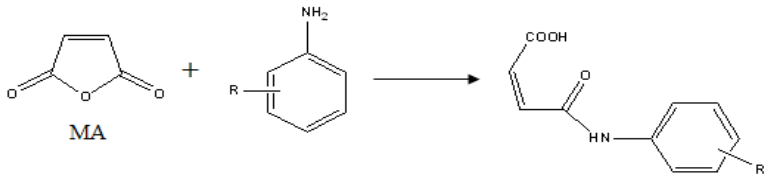

I- p-MOMA R = OCH_3
II- p-MMA R = CH_3

Scheme 1. Synthesis of maleanilic acid derivatives (I-II)

TABLE 1. Analytical data of maleanilinic acid derivatives (I-II)

Compounds	Empirical formula	m.p./ºC	Color and Yield(%)	Formula mass/ g/mol	Elemental Analysis		
					C%	H%	N%
					Found (Calc.)	Found (Calc.)	Found (Calc.)
p- MOMA	$C_{11}H_{11}NO_4$	200	Green (91)	221.21	60.71 (59.67)	5.08 (4.97)	6.41 (6.33)
p- MMA	$C_{11}H_{11}NO_3$	195	Faint yellow (96)	205	64.48 (64.39)	6.19 (5.36)	6.91 (6.82)

The structure conclusions of two novel maleanilinic acids are summarized. For simplicity, modes of vibrations of aromatic compounds are considered as separate ring C-H or C-C vibrations. However, as with any complex molecules, vibrational interactions occur and these labels only indicate the predominant vibration. Substituted benzenes have large number of sensitive bands. These bands; which position are significantly affected by the mass and electronic properties, mesomeric or inductive, of the substituents. According to the literature [21,22], in infrared spectra, most mono nuclear and poly nuclear aromatic compounds have three or four peaks in the region 3000 -3100 cm^{-1} [23], these are due to the stretching vibrations of the ring C-H bonds. Accordingly, in the present study, C-H stretching vibrations experimentally are appeared at 3090 (3020) and 3068 (2998) cm^{-1} respectively. These assigned frequencies are ordered in increasing wavenumber values as pMMA < p-MOMA. These bonds indicated the ring vibrations affected by the Hamette substituents values [24]. The spectrum of O-H of carboxylic acid group is usually appeared as broad absorption band occurring in the region from 2400 to 3400 cm^{-1} [25]. The band of carboxylic acid associated with carbonyl group C=O stretching absorption are appeared experimentally at 1702 and 1699 cm^{-1} for p-MMA and p-MOMA respectively. The N-H stretching frequency of a secondary amide consists of one band of ν 3206.74 cm^{-1} fermi resonance band with overtone of band and the band shifts to a lower frequency and appears near 1500 cm^{-1} (1517 cm^{-2}). C=O for amide stretch occurs at approximately 1650-1690 cm^{-1} [26] but present at 1630 cm^{-1}. This lower –frequency absorption is due to the resonance in the amide functional group; so stretching band of carbonyl group of cyclo-imide 1680.07cm^{-1}. Aromatic amine shows strong C-N stretching absorption in the region of 1300-1000 cm^{-1} [27] of peak at1304.67 cm^{-1}. Therefor, the higher frequency is due to the force constant of the C-N bond as increased due to resonance with the benzene ring and also N-H of secondary amine is wagging 896.17 cm^{-1}. With C-O stretching vibration band (1269 cm^{-1}) for acid as a medium intensity band, stretching vibration band at 3088 cm^{-1} due to presence of C-H sp^2, C=C of benzene ring 1597.98cm^{-1} [28,29]. These data confirmed the prepared structure of derivatives in Fig. 2.

Thermal analyses

In TA, the molecules are continuously energized and deactivated by a gas evolution

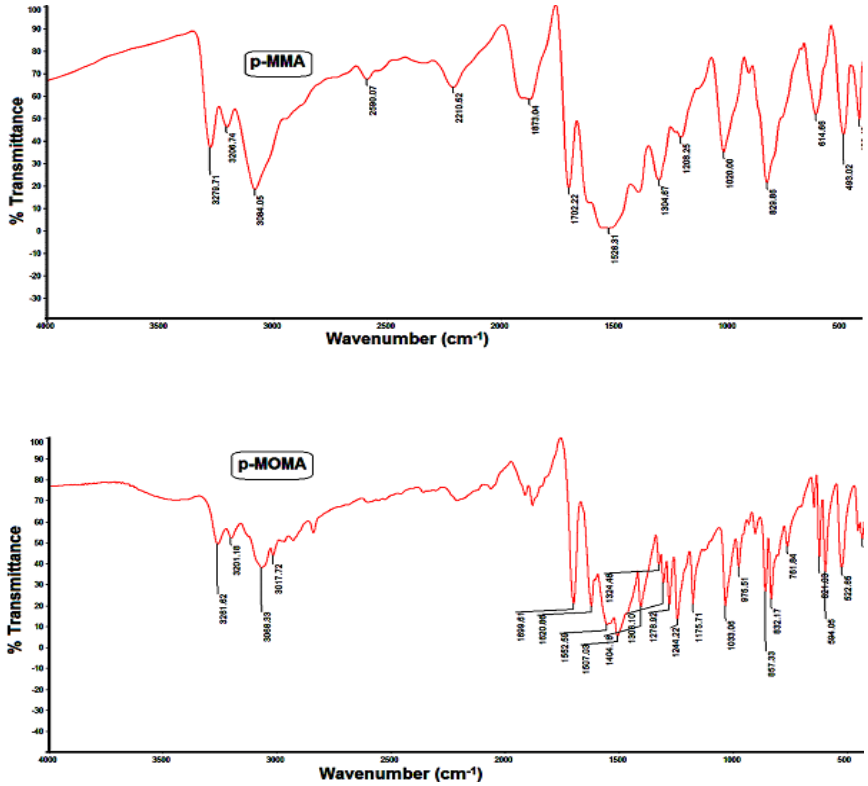

Fig. 2. The FT-IR of derivatives of maleanilinic acids (I-II)

and the distribution of energy can be described as a function of temperature. Thermogram (TG) is a technique in which the change in weight of substances is recorded as a function of temperature or time. It is represented as weight change with temperature (TG) and a derivative curve (DTG). The TG/DTA curves of the title compounds were displayed between 25 to 400°C using a heating rate (10° min^{-1}) and results obtained are given in Fig. 3 and 4.

The interpretation of these data and complete description of the thermal degradations of these derivatives are shown in Table 2.

The thermal analyses results show that both of these compounds have similar behavior. The p-methyl derivative (p-MMA) decomposed in one step as given by the TG/DTG curve (Fig. 3); while p-MOMA decomposed in two steps (Fig. 4). The steps of decomposition of the title compounds are detected and confirmed by DTA.The proposed thermal decomposition of these derivatives represented in Scheme 2.

In general, the first step is due to the broken of the bond C4-N7 position in the title compounds; which confirmed by mass losses from TG and DTG as shown in Table 3.This appears in DTA as endothermic peak and small exothermic peak that is due to chemical rearrangement to form 4-amino-4-oxobut-2-enoic acid $C_4H_5O_3N$.

For example, p-MOMA, it is clear that there are two steps. The first broken take place at the weakest bond positions. Firstly, p-MOMA losses C_7H_8O anisole molecule at C4-N7 and CH_3NO formamide molecule at C8-C10. This confirmed by mass losses from TG occurred in first step 49.95% (calculated 48.8%) within temperature range 140-205°C exactly at 186.25 °C (from DTG curve). The second step losses of CH_3NO formamide molecule; which confirmed by weight losses from TG occurred at 20.36 % (calculated 20.35 %) within temperature range 210-310 °C exactly at 306.06°C. This corresponding temperature ranges and the changes accompanying the mass loss are followed from the DTA study. In DTA curve, the first loss is referred to endothermic reactions, but

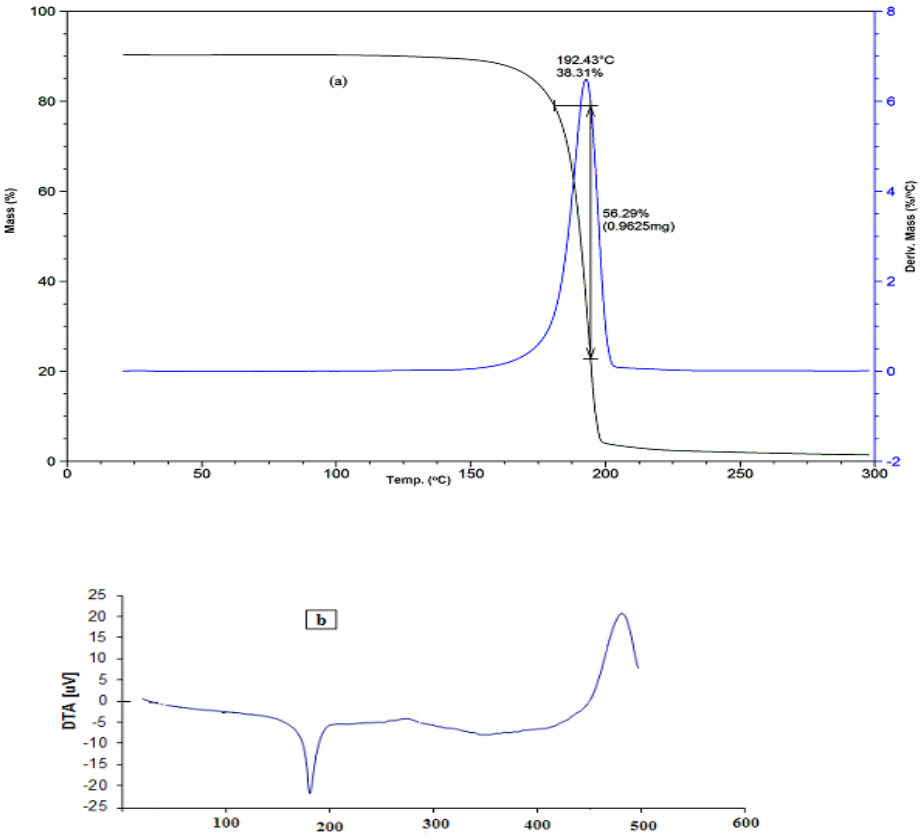

Fig. 3. Thermal analyses of p-MMA: a- TG/DTG b- DTA

TABLE 2. Thermal degradation data of the title compounds (I-II)

Compound	TGA		DTA		
	Mass.Loss pract. (calc%)	Temp range°C	Peak temp./°C	Temp. range /°C	Description
p-MMA	56.29 (56.09)	150-210	180.00 480.00	156.7-209.2 401.8-497.2	Endothermic Exothermic
p-MOMA	49.95 48.80	120-205	182.96	150.0-200.0	Endothermic
	20.36 20.35	210-310	483.55	400.0-500.0	Exothermic

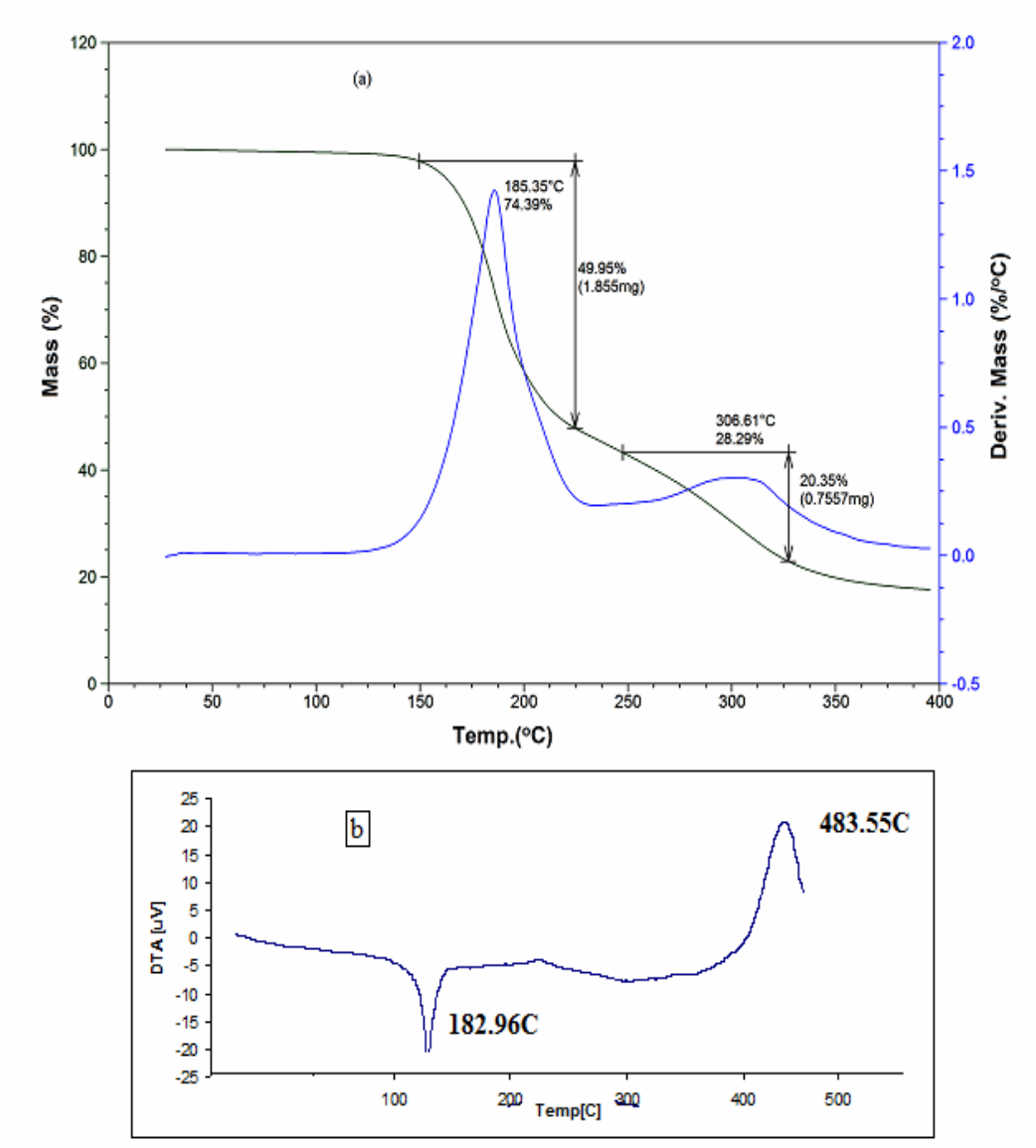

Fig. 4. Thermal analyses of p-MOMA: a- TG/DTG b- DTA

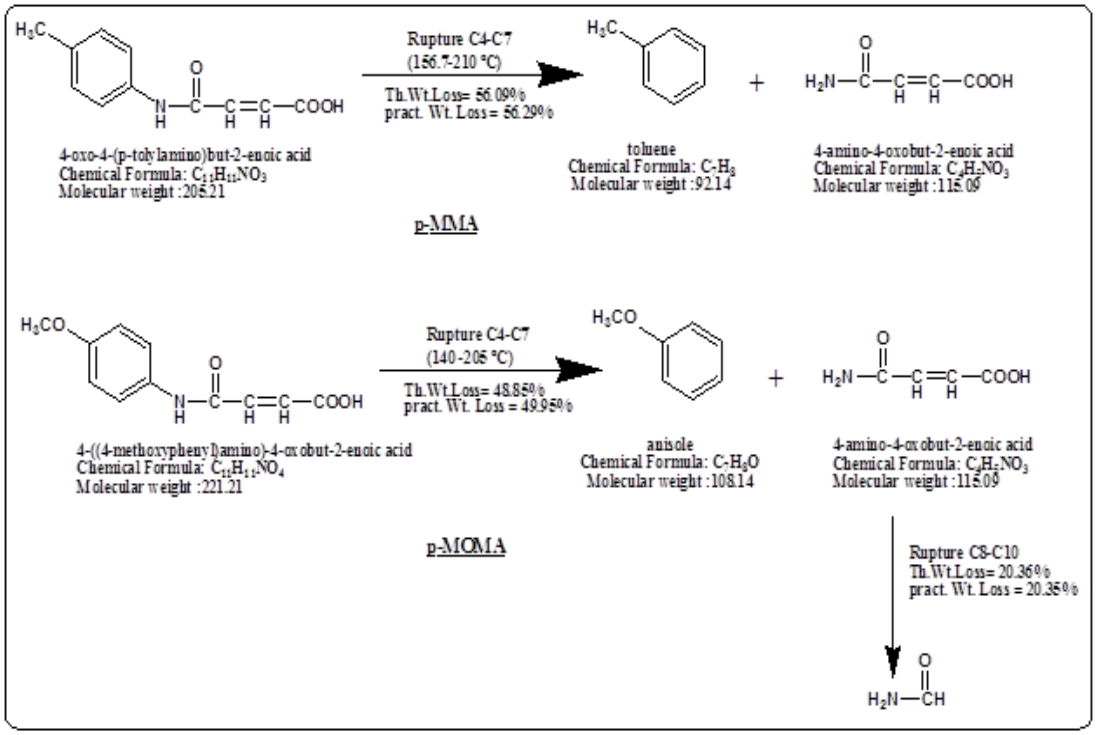

Scheme 2. Proposed thermal decomposition of derivatives

TABLE 3. Thermodynamic parameters of thermal decomposition of p-MMA and p-MOMA at different rates (5, 10 and 15)

p-MOMA							
Rate	**Decomposition Temp. Range (K)**		**E* KJ mole^{-1} first step (second step)**	**A (S^{-1}) first step (second step)**	**ΔS J.K-1.mole-1 first step (second step)**	**ΔH KJ mole-1 first step (second step)**	**ΔG KJ mole-1 first step (second step)**
	First step	**Second step**					
5	397.00-467.00	467.00-654.00	164.90 (41.20)	4.3 E+18 (4.3 E+06)	108.47 (-122.31)	161.10 (37)	112.30 (99.40)
10	409.20-479.90	479.90-645.40	159.70 (69.01)	3.7E+17 (5.3E+05)	89.85 (-140.96)	155.89 (64.19)	114.32 (145.95)
15	410.30-497.14	497.14-655.76	139.50 (58.89)	7.5 E+14 (2.5 E+05)	36.07 (-147.50)	135.52 (53.96)	118.46 (141.07)
p-MMA							
5	422.91-485.87		238.60	2.8E+26	257.74	234.70	114.80
10	423.07-510.47		182.80	3.1E+19	124.41	178.90	120.50
15	447.7.-523.34		180.20	6.9E+18	111.77	176.30	122.80

the last loss is referred to exothermic reaction. The endothermic peak may be attributed to the loss of $C_4H_5NO_3$ at the range 150-200°C that followed by exothermic peak at 400-500°C. This may refer to chemical rearrangement and/ or chemical recombination of the fragments molecules unstable that followed by chemical rearrangement to $C_4H_5NO_3$ 4-amino-4-oxobut-2-enoic acid. Coats and Redfern [30] is used to calculate thermodynamic parameters from TGA curves at different rates (5, 10 and 15); which represented in Table 3.

It is found, that ΔG, E*, ΔS and ΔH values are changed from one thermal stage to another. These results indicate that, the increasing of heating rate facilitated the decomposition of the two derivatives; which confirmed by the positive ΔH and ΔG values as endothermic processes. The positive ΔS values indicate the disorder of the obtained fragments in thermal decomposition of p-MMA as a whole and in first step of p-MOMA derivative at different heating rates. While the negative values of ΔS in second step decomposition of p-MOMA may refer to stability and great ordering of the obtained fragments. The gradual decrease in activation energy required for thermal degradation (E*) values with the increase of heating rate means that; the rate of thermal decomposition of both derivatives increases with increasing of heating rate. The obtained broken coming from thermal degradation of neutral molecule derivatives will be confirmed by molecular orbital calculations (MOCs).

Theoretical calculations

Geometry optimization

To illustrate the broken coming from thermal degradation of neutral molecule derivatives; so it is necessary to investigate the geometry change of compounds structure. The geometry optimized parameters bond length, bond order and bond angle of p-MMA and p-MOMA calculated by B3LYP/6-311++G(d, p) and HF/6-311G(d), regarding to our knowledge the experimental data on geometric structure of p-MMA and p-MOMA are not available in the literature. Therefore, the theoretical results have been compared with the experimental data on N-phenylmaleamic acid [31] as shown in Table 4.

From the theoretical values (bond length, bond order and bond angles) of p-MMA and p-MOMA, we can notice that the most of optimized bond angle (C2C1C6) is lower than the corresponding value of N-Phenylmaleamic acid. The bond angles C2C1R and C6C1R are higher than N-Phenylmaleamic acid. The values of C1-R bond (bond length and bond order) are increased in following order: p-MMA (~1. 51Å, 1.02) > p-MOMA (~1.363Å, 1.003). This difference in bond length, bond order and bond angles may be attributed to redistribution of charges on atoms of R = CH_3 and OCH_3 in the para-position of the benzene ring. This order occurs as a result of the charge redistribution; which due to substituents effects such as electronegativity, electron withdrawing and/or electron attracting abilities in form of Hamette's substituents values [24]. The optimized bond lengths of C–C in benzene ring falls in the range 1.379–1.404 Å which are in good agreement with those of experimental bond lengths [1.377-1.403 Å]. The bond length of C4-N7, C8-C10 and C11-C12 are more elongated than other bonds; which also is in agreement with N-Phenylmaleamic acid bond length. The bond length C4-N7 elongation is due to delocalization charges on benzene ring. The bond lengths C8-C10 and C11-C12 elongation are due to the withdrawing effect of O9 and N7 on C8 atom and effect O13and O14 on C12 atom. Consequently, the loss of any part of the studied compounds during either thermal or mass fragmentation is mainly related to the elongation of these bonds.

Frontier molecular orbitals (FMOs)

The knowledge of frontier orbitals is important for determining the reactivity of molecules. Therefore, energies of highest occupied molecular orbital (HOMO) and lowest unoccupied molecular orbital (LUMO) of the title compounds are calculated using theories and their basis sets, HF/6-311G (d) and DFT/B3LYP/6-311G++(d,p). According to Koopman's theorem [32], the ionization energy (I) and electron affinity (A) related to the energies of HOMO and LUMO as $I = -E_{HOMO}$ and $A = -E_{LUMO}$. These orbitals determine the way the molecule interacts with other species; where HOMO represents the ability of the molecule to donate an electron whereas LUMO represents ability of molecule to accept an electron. The frontier orbital energy gap (The energy difference between HOMO and LUMO) helps to characterize the chemical reactivity and kinetic stability of the molecule. A molecule with a small frontier orbital gap is more polarizable and is generally associated with a high chemical reactivity, low kinetic stability and is also termed as soft molecule [32]. Alternatively, the chemical hardness and softness of a molecule are good

TABLE 4. Optimized geometric parameters for p-MMA and p-MOMA computed at HF with 6-311G(d) and at DFT(B3LYP) with 6-311++G (d, p) basis sets.

	p-MMA		p-MOMA		Exp. N-phenylmaleamic acid
	HF/6-311g(d)	B3LYP/6-311++G(d,p)	HF/6-311g(d)	B3LYP/6-311++G(d,p).	
			Bond length(Å)*		
C1-C2	1.390	1.400	1.383	1.397	1.403
C1-C6	1.385	1.397	1.390	1.399	1.377
C1-R	**1.510**	**1.509**	**1.348**	**1.364**	**0.950**
C2-C3	1.379	1.388	1.388	1.393	1.377
C3-C4	1.391	1.402	1.382	1.397	1.403
C4-C5	1.387	1.400	1.395	1.404	1.387
C4-N7	**1.412**	**1.412**	**1.415**	**1.413**	**1.419**
C5-C6	1.387	1.393	1.377	1.386	1.403
N7-C8	1.357	1.376	1.355	1.375	1.350
C8-O9	1.192	1.220	1.193	1.221	1.249
C8-C10	**1.501**	**1.496**	**1.501**	**1.495**	**1.476**
C10-C11	1.318	1.336	1.318	1.336	1.335
C11-C12	**1.485**	**1.477**	**1.485**	**1.477**	**1.496**
C12-O13	1.181	1.208	1.181	1.208	1.277
C12-O14	1.329	1.360	1.329	1.360	1.307
O15-C16	----	----	1.398	1.421	---
			Bond order*		
C1-C2	1.3864	1.3849	1.4065	1.372	---
C1-C6	1.4180	1.4031	1.3503	1.349	---
C1-R	**1.0195**	**1.0335**	**0.9660**	**1.003**	---
C2-C3	1.4556	1.4619	1.4019	1.433	---
C3-C4	1.3685	1.3592	1.4172	1.382	---
C4-C5	1.3935	1.3654	1.3481	1.339	---
C4-N7	**1.0027**	**1.0430**	**0.9969**	**1.039**	---
C5-C6	1.4205	1.4409	1.4765	1.476	---
N7-C8	1.1211	1.1444	1.1277	1.149	---
C8-O9	1.6433	1.6494	1.6372	1.643	---
C8-C10	**0.9882**	**1.0177**	**0.9880**	**1.019**	---
C10-C11	1.8942	1.8297	1.8940	1.827	---
C11-C12	**1.0047**	**1.0402**	**1.0049**	**1.041**	---
C12-O13	1.7277	1.7469	1.7275	1.746	---
C12-O14	0.9897	1.0224	0.9894	1.022	---
O15-C16	---	---	0.8976	0.909	---
			bond Angle (Å)*		
C2C1C6	**117.327**	**117.4697**	**118.830**	**119.171**	**120.0**
C2C1R	**121.030**	**121.1047**	**124.961**	**124.7167**	**120.0**
C6C1R	**121.635**	**121.4151**	**116.207**	**116.1124**	**120.0**
C1C2C3	121.223	121.2015	119.735	119.6399	119.9
C2C3C4	120.703	120.5824	121.514	121.2842	120.3
C3C4C5	118.950	119.0745	118.639	118.8968	119.8
C3C4N7	117.036	117.3364	117.532	117.6364	116.4
C5C4N7	124.012	123.5887	123.828	123.4669	**128.8**
C4C5C6	119.412	119.3591	119.818	119.7765	119.3
C1C6C5	122.383	122.3118	121.462	121.2317	120.6
C4N7C8	128.891	129.1684	128.856	129.085	128.0
N7C8O9	125.163	124.5423	125.183	124.5241	122.3
N7C8C10	112.976	112.8191	112.996	112.8449	114.5
O9C8C10	121.859	122.6386	121.819	122.6309	123.1
C8C10C11	120.312	120.6292	120.321	120.6295	128.4
C10C11C12	123.671	124.2988	123.669	124.3199	**132.0**
C11C12O13	123.282	123.9645	123.300	123.9939	118.1
C11C12O14	113.943	113.6486	113.950	113.6768	120.7
O13C12C14	122.774	122.3869	122.748	122.3292	121.2
C1C15C16	---	---	119.693	118.5942	---

* The assigned values are discussed

indicators for the chemical reactivity of a given molecule; which can calculate from energy gap. The soft molecule is more polarizable than the hard one because it needs small energy to excitation. Softness (S) is a property of molecule that measures the extent of chemical reactivity. It is defined as the reciprocal of hardness (**η**) and **η** = (I - A)/2 [33]. HOMO and LUMO orbitals are shown in Fig. 5.

As shown in Fig. 5, the p-MOMA compound has less energy gap (2.60eV of HF and 3.398eV of B3LYP), thus it is more reactive and softer (0.769 of HF and 0.572 of B3LYP) than the p-MMA (0.649of HF and 0.542of B3LYP) compound. In addition, the chemical potential (μ) and electronegativity (**χ**) of a molecule can be calculated as follows: μ = -(I + A)/2, and **χ** = (I + A)/2, i.e. μ = - **χ**. The electrophilicity index (**ω**), $x = \mu^2/2\eta$, [34] is a measure of energy lowering due to maximal electron flow between donor and acceptor, which indicated that there is similarity for two derivatives.

The substituents (R= OCH_3 and CH_3) of title compounds can influence reactivity of molecules; which increased molecular dipole moments as a result of increasing electrophilicity of the substituent. Electrophilic substitution may be correlated with the electron donating or electron withdrawing. The calculated molecular dipole moments by both HF and DFT theories are found to be dependent on the electron donating power of Hammett substituents and they are presented in the following order: p-MMA (4.954D) < p-MOMA (6.257D) of HF and p-MMA (5.159D) < p-MOMA (6.543D) of DFT/B3LYP. From these data it is concluded that, the p-MOMA is more reactive and polarizable compound than the p-MMA.

Natural Bond Orbitals (NBO) Atomic Charges

NBO atomic charges calculation has an important role in the application of quantum

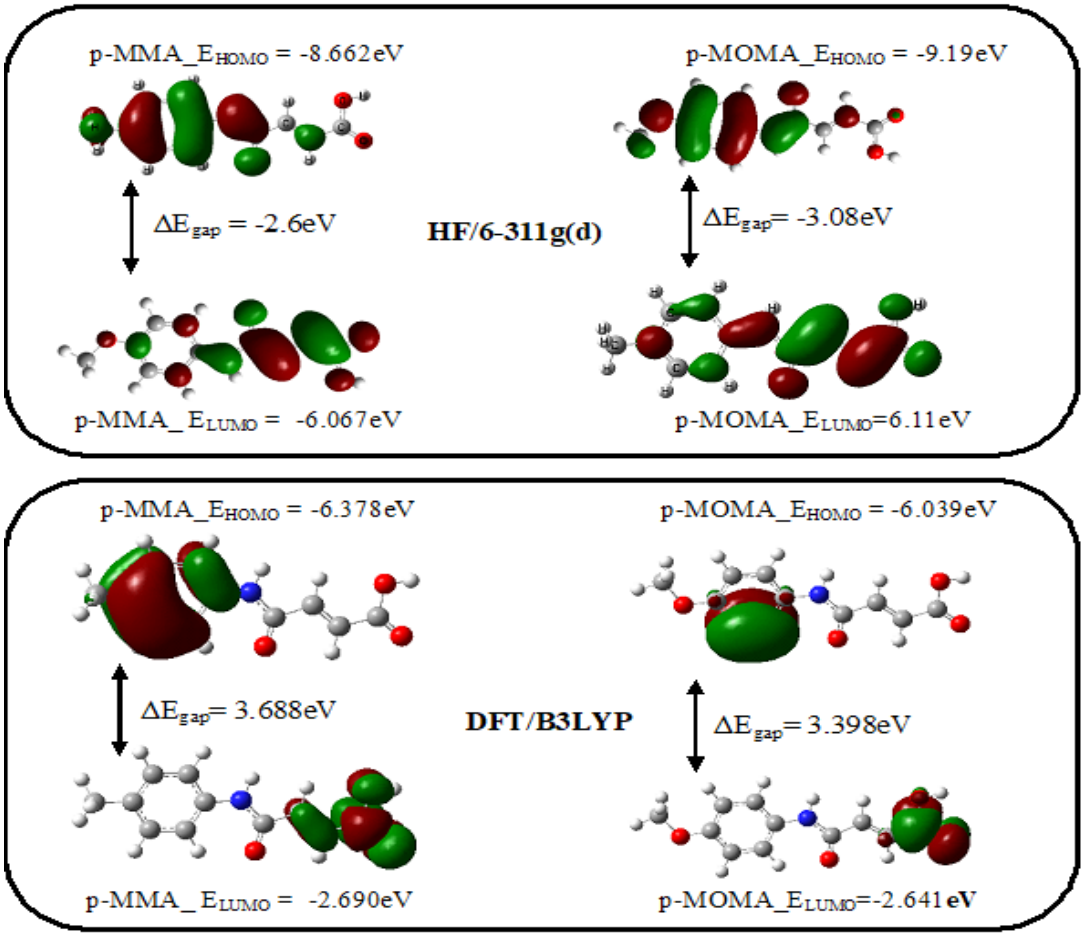

Fig. 5. Molecular orbital surfaces and energy levels of the studied compounds.

chemical calculation to molecular system; because atomic charges affect dipole moment, molecular polarizability, electronic structure, and a lot of properties of molecular systems [35]. The charge distribution over the atoms suggests the formation of donor and acceptor pairs involving the charge transfer in the molecule (Fig. 5). Atomic charge has been used to describe the processes of electronegativity equalization and charge transfer in chemical reactions [36,37]. In case of p-MOMA the charge on C1 (0.36586e of HF and 0.31495e of B3LYP) is positive compared with charge on C1 (-0.03740e of HF and -0.03969e of B3LYP) in case p-MMA molecules. This is due to OCH_3 substituent effect. Also, the charge on C4 atom of both p-MMA (0.19042e of HF and 0.14399e B3LYP) and p-MOMA (0.15815e of HF and 0.12482e of B3LYP) has a positive charge. Likewise, C8 atom (~0.81e of HF and ~0.63e of B3LYP) and C12 atom (0.93e of HF and ~0.76e of B3LYP) possess the maximum positive charge among all carbon atoms in p-MMA and p-MOMA compounds. This is due the withdrawing effect of O9 and N7 on C8 and C4 atom and effect of O13 and O14 on C12 atom. It is confirmed by low charge density on C10 atom (~ -0.23e of HF and ~ -0.21e of B3LYP), and on C11 atom (-0.23eof HF and ~ -0.23e of B3LYP). This withdrawing effect causes elongation of the bonds C8-C10, C11-C12 and C4-N7 respectively.

From the values of partial charges (Fig. 6) on atoms we notice that there is a repulsive force of C1-R and C4-N7 in p-MMA molecule and

TABLE 5. Calculated energy values, chemical hardness, electro negativity and chemical potential of p-MMA and p-MOMA at HF with 6-311G (d) basis set.

	p-MOMA		p-MMA	
	HF	**B3LYP**	**HF**	**B3LYP**
	6-311g(d)	6-311++G(d,p)	6-311g(d)	6-311++G(d,p)
E_{total}(Hartree)	-777.05	-781.97	-702.19	-706.44
E_{HOMO} (eV)	-8.662	-6.039	-9.19	-6.378
E_{LUMO}(eV)	-6.067	-2.641	-6.11	-2.690
$E_{HOMO-LUMO}$ (eV)	-2.60	-3.398	-3.08	-3.688
Chemical hardness (η)	1.3	1.749	1.54	1.844
Electronegativity (x)	7.37	4.34	7.65	4.534
Chemical potential (μ)	-7.37	-4.34	-7.65	-4.534
Chemical softness(S)	0.769	0.572	0.649	0.542
Dipole moment(D)	6.257	6.543	4.954	5.159

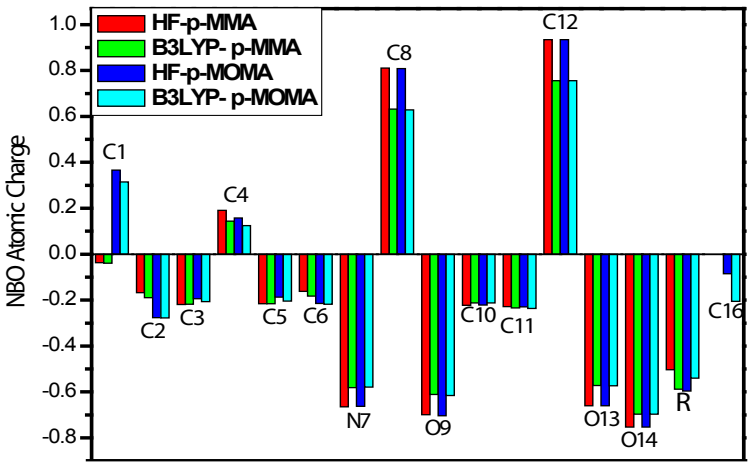

Fig. 6. NBO atomic charges of p-MMA and p-MOMA molecules calculated at HF/6-311G(d) and DFT/B3LYP/6-311++G(d,p) level of theory

attractive force in p-MOMA. But in both p-MMA and p-MOMA there are attractive forces of C8-C10 and C11-C12 bond atoms.

Natural bonding orbitals analysis

The natural bonding orbitals (NBO) analysis can show an efficient way for describing intra and inter-molecular bonding and interactions between bonds. Also, it is a convenient way to investigate charge transfer or hyper-conjugative interactions in the molecular system [38]. The hyper-conjugative is given as stabilizing affects that due to overlapping between an occupied (filled) orbital with another unoccupied (empty) orbital. NBO analysis has been calculated on p-MMA and p-MOMA at DFT/B3LYP/6-311++G(d,p) method to investigate the intra and inter-molecular interaction and delocalization of electron density.

Molecular electronic potential maps

The molecular electrostatic potential (MEP) is best suited for identifying sites for intra- and intermolecular interactions [39]. In compound-receptor, it is a very useful descriptor in understanding sites for electrophilic and nucleophilic reactions [40]. To predict reactive sites of the investigated p-MMA and p-MOMA molecules; the molecular electrostatic potential (MEP) was calculated with B3LYP/6-311++G(d,p) for the optimized geometries by using the Gauss View 5 software. The MEP maps of p-MMA and p-MOMA are shown in Fig. 7. So there are different values of the electrostatic potential at the MEP surface are represented by different colors. Therefore, the shades of red represent the regions of electronegative electrostatic potential; the shades of blue show the regions of the positive electrostatic potential and the green color illustrates the regions of zero potential. The potential increases in the following order: red<orange<yellow<green<blue. The maximum negative region (red color) determines the site for electrophilic attack whereas the maximum positive region (blue color) indicates the site of nucleophilic reaction.

In the case of the p-MMA structure, the limit of the molecular electrostatic potential is ±0.119 a.u

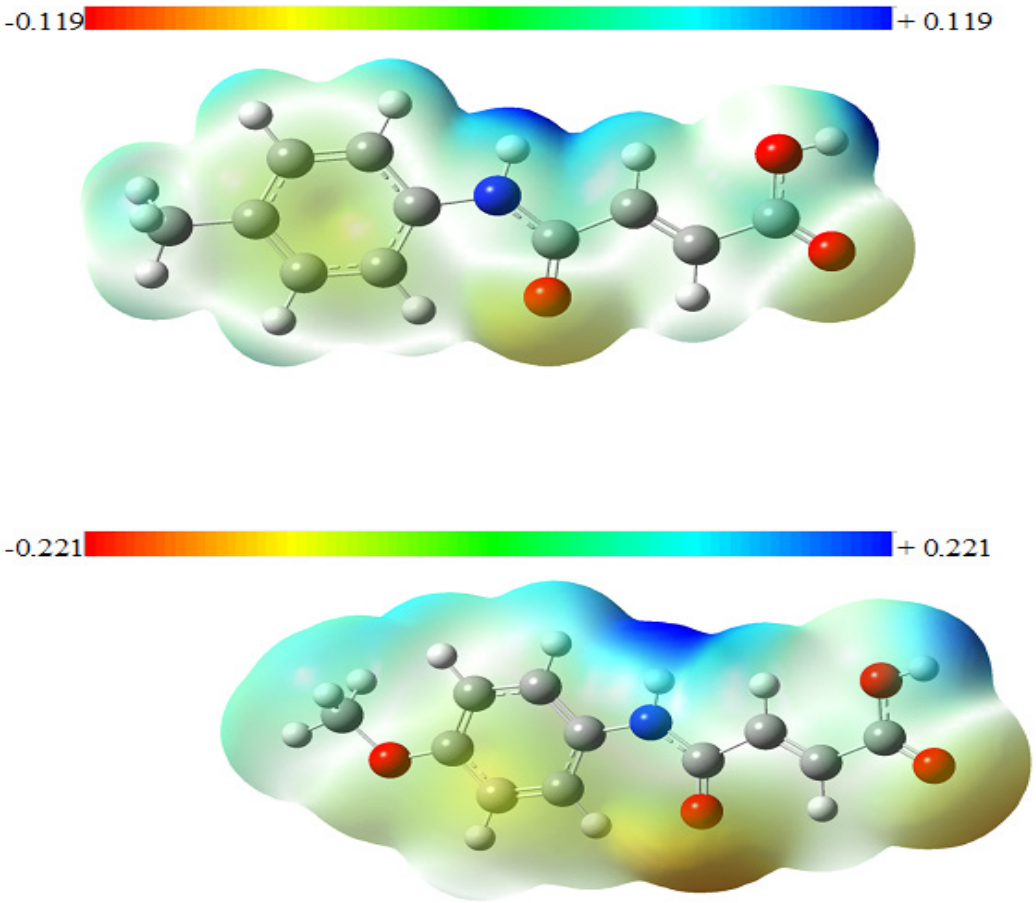

Fig. 7. Molecular electrostatic potential map (MEP) of p-MMA and p-MOMA

and ±0.221 a.u of p-MOMA. The carbonyl (C=O) atoms reflect the most electronegative region (orange regions) and show medium nucleophilic activities due to negative charge excess, it can be proven as a favored site of electrophilic attack. The H20 and H23 atoms have positive charge (dark blue region); which can be acted as centers for several inter H-bond with other molecules.

Correlation of the TA behavior, DFT calculations, and NBO analysis of the neutral p-MMA and p-MOMA molecules

In literature there is no study on the thermal stability of these compounds with temperature changes. The determination of initial bond cleavage would be an important first step in using these calculations in a predicative manner [41]. The occupancies and energies of bonding molecular orbital of p-MMA and p-MOMA compounds are given in Table 6.

On the basis of these computational data of B3LYP/6-311++G(d,p) calculation for the p-MMA and p-MOMA molecules; there are C4–N7, C8-C10 and C11-C12 bonds have average larger bond length (1.412Å, 1.50Å and 1.475Å) and average lower bond order (1.02, 1.00 and 1.03) respectively. Otherwise, C1-R of p-MMA has lager bond length (1.51 Å) with lower bond order (1.00) compared to p-MOMA molecule. The electrostatic attraction forces between C4 (0.12482) and C7 (-0.57902) are smaller than that between C8 (0.62880) and C10 (-0.21229) and between C11(-0.23581) and C12(0.75575) from Fig. 7. Also, from Table 9, the bond energies of bond C1-R and C4-C7 are lower than that of bonds C8-C10 and C11-C12.

Interestingly, from our point of view, it is expected that the C4-N7 bonds are first bond cleavage because of i) small difference in bond length and bond order between the bonds. ii) The electrostatic attraction between C4 (0.12482) and C7 (-0.57902) are lower than between C8(0.62880) and C10(-0.21229) and between C11(-0.23581) and C12(0.75575) iii) Bond energies of C4-C7 are lower than C8-C10 and C11-C12; iv) Strong stabilization of benzene and $C_4H_5O_3N$ moiety because of there are large delocalized electrons from NBO analysis. The explanations obtained by DFT calculations and NBO analysis are in agreement with the TA degradation. This is clear because the p-MMA and p-MOMA molecules decomposed to loss (C_7H_8O) anisole molecule at C4-N7 and (CH_3NO) formamide molecule at C8-C10; which confirmed by weight losses from TG occurred in first step 49.95% (calculated 48.8%) within temperature range 140-205^{o}C exactly at 186.25 °C (from DTG curve). The second step losses of CH_3NO formamide molecule; which confirmed by weight losses from TG occurred at 20.36 % (calculated 20.35 %) within temperature range 210-310 ^{o}C exactly at 306.06^{o}C that corresponding temperature ranges and the changes accompanying the weight loss are followed from the DTA study.

XRD characterization

The powder X-ray diffraction (XRD) profiles are obtained for both two derivatives; which have main sharp peaks are identified at angles (2θ) and (d-spacing) for p-MMA and p-MOMA (Fig. 8).

The diffraction data was recorded for 2Θ values between 10^o and 70^o. The comparison between the XRD patterns of two derivatives and maleimide show a degree of 2θ (27^o) of maleimide as pattern of derivatives. The patterns of two derivatives have two high intensity peaks for p-MMA 4462 (18.44^o), 777.08(27.08^o) and 235.56(18.44^o), 1866 (27.08) and p-MOMA respectively. The difference in d-spacing (^{o}A) values of the studied molecules for electron donating decreases in the order: p-MMA (19.31) > p-MOMA (11.22); which is in good agreement with Hammett substituents values [24]. The quantitative elemental analysis of X-ray energy dispersive spectroscopy was mainly used for confirming the presence of substituent atoms in para position on the benzene ring. These results refer to high degree crystallinity of both

TABLE 6. The occupancies and energies of bonding molecular orbital of p-MMA and p-MOMA compounds

Atomic orbital	Occupancy (e)		Bond Energy (a.u.)	
	MOMA	MMA	MOMA	MMA
C1-R	1.99184	1.98269	-0.90822	-0.63241
C4-C7	1.98747	1.98763	-0.86602	-0.8184
C8-C10	1.97570	1.97579	-0.67759	-0.6790
C11-C12	1.97879	1.97877	-0.30465	-0.6991

derivatives. As a result of correlating these data it revealed and confirm good correlation between experimental (TA and XRD) and theoretical HF/6-311G(d) and DFT/B3LYP/6-311++G(d,p) level of theory calculations.

Cytotoxicity

Assessment of growth inhibitory effect of p-MMA and p-MOMA on HCT-116 cell, MCF-7 cell and HepG-2 cell; in the order of increasing dosages of p-MMA and p-MOMA extract are disruptive against Colon carcinoma cells, Breast carcinoma and Hepatocellular carcinoma. The obtained results are depicted in Fig. 9.

It can be concluded that; the inhibitory activities of p-MMA and p-MOMA with IC50 values under these experimental conditions against Breast

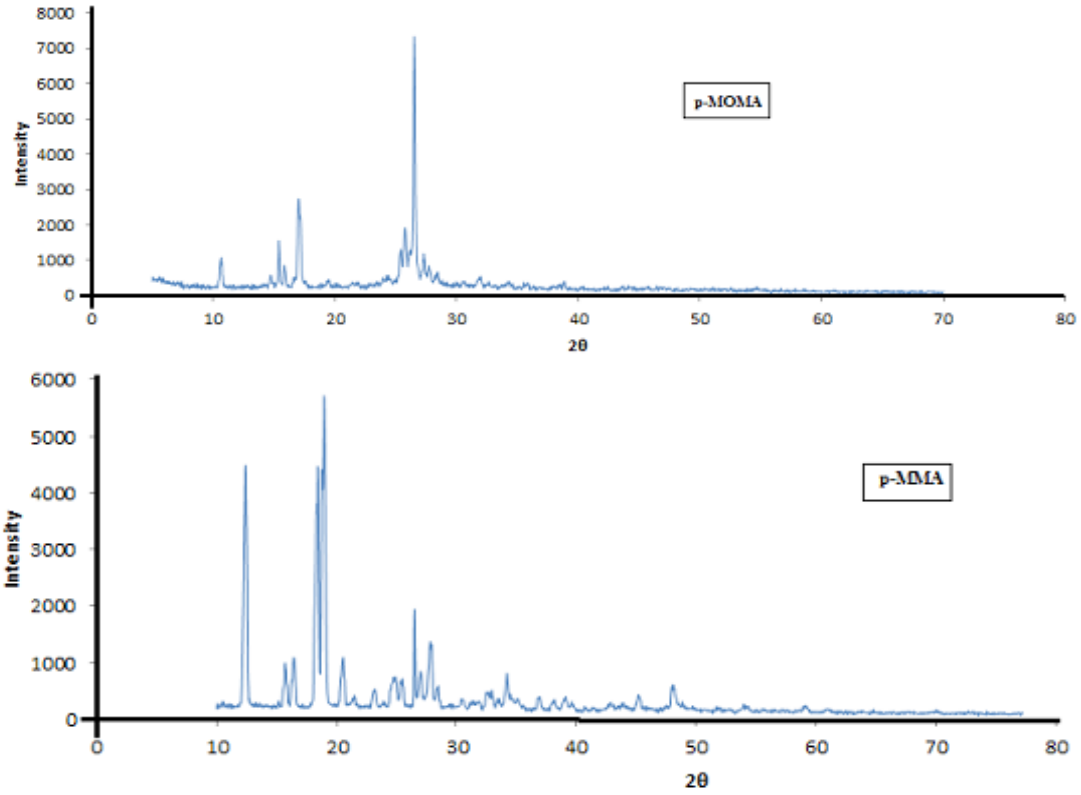

Fig. 8. X-ray diffraction data for p-MMA and p-MOMA derivatives

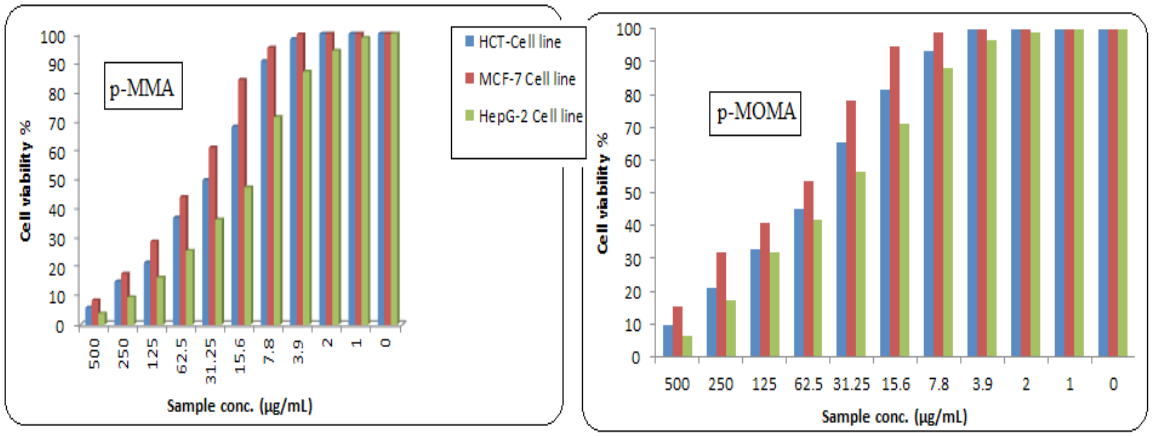

Fig. 9. The effect of p-MMA and p-MOMA on: *HCT-116 cell*, *MCF-7 cell* and HepG-2 cell

carcinoma cells are detected at 51.3 and 81 µg / mL respectively. Whereas against Hepatocellular carcinoma cells the inhibitory values are detected at 14.7 and 44.7 µg / mL respectively; also against colon carcinoma cells the inhibitory values are detected at 31 and 54.9 µg / mL respectively. Therefore; p-MMA and p-MOMA are highly effective against Hepatocellular carcinoma cells > colon carcinoma cells > Breast carcinoma cells. It is now recognized, that cancer cells over expression promotes tumorigenic functions; which can be suppressed by p-MMA and p-MOMA inhibitors.

These data refer to cytotoxicity of p-MOMA is found to be more toxic for the three kinds of carcinoma cells (81, 44.7 and 54.9 µg / mL) than p-MMA (51.3, 14.7 and 13 µg / mL). The high cytotoxicity of p-MOMA can be rationalized and correlated with theoretical calculations. The pronounce cytotoxicity of p-MOMA may be attributed to the calculated molecular dipole moments by both HF and DFT theories; which are found to be dependent on the electron donating power of Hammett substituents and they are presented in the following order: p-MMA (4.954D) < p-MOMA (6.257D) of HF and p-MMA (5.159D) < p-MOMA (6.543D) of DFT/B3LYP. From these data it is concluded that, the p-MOMA is more reactive and polarizable compound than the p-MMA. The molecular electrostatic potential (MEP, Fig. 7) referred to the more possible intra- and intermolecular interactions [39] of p-MOMA molecule to carcinoma cells than p-MMA as confirmed by molecular electrostatic potential values of ±0.221 a.u for p-MOMA and ±0.119 a.u for p-MMA.

Conclusion

This work involved preparation of new compounds p-MOMA and p-MMA by solvent free reaction between maleic anhydride and methyl and methoxy aniline derivatives at room temperature and characterized by different physico-chemical techniques. This new approach, solvent free preparation method is simple, clean, economic and nearly quantitative or high yield. The experimental studies were complemented by molecular orbital calculations at DFT/ B3LYP method and HF with 6-311++G (d,p) basis set with 6-311G(d) basis set, respectively. Calculations were carried out using GAUSSIAN 09 suite of programs. The molecular geometry parameters are generally agreed with the N-phenylmaleamic acid experimental values. The geometry optimization of studies molecules showed that bond lengths C1-R, C4-N7, C8-C10 and C11-C12 are longer bond length and C1-R for p-MMA compound is longest bond length (weakest bond) between both molecules. This is mainly due to attachment of electro-negative oxygen (O9, N7, O13 and O14). From total energy and dipole moment we estimated p-MOMA compound is higher reactivity with less stability. Also, these data confirmed from HOMO and LUMO energy gaps. NBO calculations show that there is a strong delocalized electron on the aliphatic parts $C_4H_5NO_3$ and benzene ring of both studied compounds and consequently increase of stability of these parts.

Cytotoxicity

The results obtained of cytotoxicity studies indicate that:

Inhibitory activity of p-MMA against Breast carcinoma cells was detected under the experimental conditions and found to be IC50 = 51.3µg/mL < against Colon carcinoma cells and found to be in the order IC50 = 31 µg/mL < against Hepatocellular carcinoma cells and found to be IC50 = 14.7 µg/mL. Inhibitory activity of p-MOMA against Breast carcinoma cells was detected under these experimental conditions and found to be in the order IC50 = 81 µg/mL < against colon carcinoma and found to be in the order IC50 = 54.9 µg/mL < Inhibitory activity against Hepatocellular carcinoma and found to be IC50 = 44.7 µg/mL. Therefore; p-MMA and p-MOMA are highly effective against cancer cells in the following order: Hepatocellular carcinoma cells> colon carcinoma cells > Breast carcinoma cells and p=MOMA is more effective than p-MM as confirmed by TA and theoretical calculations.

Acknowledgments

The authors acknowledge the supports via providing chemicals, wears, instrumental measurements and lab space presented by ministry of military production Laboratories and Chemistry Department, Faculty of Science, Cairo University

References

1. Cava M. P., Deana A. A., Muth K., Mitchell, M. J., N-Phenylmaleimide, *Org. Syn.* **41,** 63 (1961).
2. Khan M. I., Baloch M. K., Ashfag M., Gull Braz, S. J., Organotin(IV) Esters of 4-Maleimido-benzoic Acid: Synthesis, Characterization and in vitro Anti-leishmanial Effects, *Chem. Soc*. **20,** 341 (2009).
3. Gowda S. K. N., Mahendra K. N., The Effect of

Surface Modification of Silica Nanoparticles on the Morphological and Mechanical Properties of Bismaleimide/Diamine Matrices. *Iran. Polym. J.* **16**, 161 (2007).

4. Fles D., Vukovic R., Kuzmic A.E., Bogdanic G., Pilizota V., Karlovic D., Markus K., Wolsperger K., Vikic D., Croat., Synthetic Methods of Organometallic and Inorganic Chemistry. *Chem.* **67**, 267 (1999).
5. Roth M., N-Phenyl-maleic acid amides for regulating the growth and development of plants. US Pat. 4125398 (1978).
6. Ryttel A.D., Angewan, Makromol., N-(p-Bromophenyl)maleimide and its copolymers with alkyl methacrylates. *Chem*. **67,** 267 (1999).
7. Corrie J.E.T.J., Thiol-reactive fluorescent probes for protein labeling, *Chem. Soc. Perkin Trans.* I 2975 (1994).
8. Fujinami A., Ozaki T., Nodera K., Tanaka K., Effect of Methyl Groups on Cyclopropane Ring on Antifungal Activity of N-(3, 5-cyclopropanedicarboximides, *Agric. Biol. Chem.* **36,** 318 (1972).
9. BodyP.D.W.,J.B.,C.E.F.,Rickard,[7,16-Bis(benzyloxycarbonyl)-6,18,15,17-tetramethyldibenzo[b,i][1,4,8,11] tetraazacyclo-tetradecinato-kappa N-4]nickel(II). *Acta Cryst.* **62,** 2734 (2006).
10. Griffiths D.G., Partice M. G., Sharp, R. N.; Beechey, R. R.; FEBS Lett., 134, 261; Morder, L.; Biol. Chem. Hoope-Seyler 1987, 368, 855; Rich, D. H.; Gasellchen, P. G.; Tong, A.; Cheung, A.; Buckner, C. K.; J. Med. Chem. 1975, 18, 1004; Codecik, E.; Reddi, K. K.; Nature 1951, 168, 475; Keller, O.; Rudinger, J.; Helv. Chim. Acta 1975, 58, 531; Nath, M.; Pokharia, S.; Yadav, R.; Coord. Chem. Rev. 2001, 215, 99; Gielen, M.; Appl. Organomet. Chem. 2002, 16, 481; Chandrasekhar, V.; Najendran, S.; Baskar, V.; Coord. Chem. Rev. 1 235 (1981).
11. Mulholland P., Dundas, D., High order harmonic generation from highly excited states in acetylene, *physical review A* (2018).
12. Mura P., Faucci M.T., Maestrelli F., Furlanetto S., Pinzauti S., *J. Pharm. Biomed. Anal.,* **1015,** 29 (2002).
13. Zayed E. M., Zayed M. A., Fahim A.M. and El-Samahy F.A. *Appl Organometal Chem*., **31**, e3694 (2017).
14. Becke A.D., Density functional thermochemistry. III. The role of exact exchange. *J Chem Phys.* **98** 5648–52 (1993).
15. Lee C., Yang W., Parr R.G., Development of the Colle–Salvetti correlation-energy formula into a functional of the electron density. *Phys Rev* B. **37,** 785–789 (1998).
16. Nassar M.Y., El-Shahat M.F., Khalile S.M., El-Desawy M., Eman A. Mohamed, *Journal of Thermal Analysis and Calorimetry,* **117,** 463-471 (2014).
17. Frisch, M.J., GW. Trucks, HB. Schlegel, GE. Scuseria, MA. Robb, JR. Cheeseman, G. Scalmani, V. Barone, B. Mennucci, GA. Petersson, H.Nakatsuji, Caricato M, Li X, Hratchian HP, Izmaylov AF, Bloino J, Zheng G, Sonnenberg JL, Hada M, Ehara M, Toyota K, Fukuda R, Hasegawa J, Ishida M, Nakajima T, Honda Y, Kitao O, Nakai H, Vreven T, Montgomery JA Jr, Peralta JE, Ogliaro F, Bearpark M, Heyd JJ, Brothers E, Kudin KN, Staroverov VN, Keith T, Kobayashi R, Normand J, Raghavachari K, Rendell A, Burant JC, Iyengar SS, Tomasi J, Cossi M, Rega N, Millam JM, Klene M, Knox JE, Cross JB, Bakken V, Adamo C, Jaramillo J, Gomperts R, Stratmann RE, Yazyev O, Austin AJ, Cammi R, Pomelli C, Ochterski JW, Martin RL, Morokuma K, Zakrzewski VG, Voth GA, Salvador P, Dannenberg JJ, Dapprich S, Daniels AD, Farkas O, Foresman JB, Ortiz JV, Cioslowski J, Fox DJ.Gaussian 09. Revision C01. Wallingford: Gaussian Inc. (2010).
18. Glendening E.D., Badenhoop J.K., Reed A.E., Carpenter J.E. and F. Weinhold F., NBO. Version 3.1. Madison: Theoretical Chemistry Institute, University of Wisconsin (1995).
19. Mosmann T., Rapid colorimetric assay for cellular growth and survival: application to proliferation and cytotoxicity assays. *J. Immunol. Methods*, **65** 55-63 (1983).
20. Gomha S.M., Riyadh S.M. Mahmmoud E.A., Elaasser, Synthesis and Anticancer Activities of Thiazoles, 1,3-Thiazines, and Thiazolidine Using Chitosan-Grafted-Poly(vinylpyridine) as Basic Catalyst. *Heterocycles,* **91**(6), 1227-1243 (2015).
21. Socrates G.; *Infrared and Raman Characteristic Group Frequencies,* 3rd edition, Wiley, New York, USA (1996).
22. Eazhilarasi G., Nagalakshmi R., Krishnakumar V.; Studies on crystal growth, vibrational and optical properties of organic nonlinear optical crystal:

p-aminoazobenzene. *Spectrochim Acta A* **71,** 502-507 (2008).

23. Varsanyi G., Assignments of Vibrational Spectra of Seven Hundred Benzene Derivatives (1974).

24. Hansch C. and Leo A., *"Substituent Constants for Correlation Analysis in Chemistry and Biology,"* Wiley-Interscience, NY (1979).

25. (a) Ellzy M.W., J.O. Jensen, H.F. Hameka, J.G. Kay, D. Zeroka, Spectrochim. Acta 57A 2417 (2001); (b) J.O. Jensen, A. Banerjee, C.N. Merrow, D. Zeroka, J.M. Lochner, *J. Mol. Struct.: Theochem.* **531,** 323 (2000).

26. Kalsi P.S., *Spectroscopy of Organic Compounds,* 5th edition (2003).

27. Donald L. Pavia, Gary M. Lampman and George S. Kriz. *Introduction to Spectroscopy*, second edition (1979).

28. Sundaraganesan N., Ilakiamani S., Saleem H., Wojciechowski P. M., Michalska D., FT-Raman and FT-IR spectra, vibrational assignments and density functional studies of 5-bromo-2-nitropyridine. *Spectrochim Acta A Mol Biomol Spectrosc.* **61,** 2995-3001 (2005).

29. Sathyanarayana D.N., *Vibrational Spectroscopy Theory and Application,* 2nd edition, New Age International (P) Limited Publishers, New Delhi, India (2004).

30. Coats A.W., Redfern J.P., Kinetic parameters from Thermogravimetric data, *Nature* **201** (4914), 68 (1964).

31. Kong Mun Lo and Seik Weng Ng., N-Phenyl-maleamic acid, *Acta Cryst.* E65, 01101 (2009).

32. Koopmans T.A. über die zuordnung von wellenfunktionen und eigenwerten zu den einzelnen elektronen eines Atoms. *Physica. Elsevier.* **1** (1-6), 104-113 (1934).

33. Chermette H., Chemical reactivity indexes in density functional theory, *J. Comp. Chem.* **20** (1), 129–154 (1999).

34. Parr R.G., Yang W., Density functional approach to frontier- electron theory of chemical reactivity, *J. Am. Chem. Soc.* **106,** 4049 (1984).

35. Sidir I., Sidir Y.G., Kumalar M., Tasal E., Ab initio Hartree-Fock and density functional theory investigations on the conformational stability, molecular structure and vibrational spectra of 7-acetoxy-6-(2,3-dibromopropyl)-4,8-dimethyl -coumarin molecule. *J. Mol. Struct.,* **964**, 134–151 (2010).

36. Jug K., Maksic Z.B., *Theoretical Model of Chemical Bonding,* Ed. Z.B. Maksic, Part 3, Springer, Berlin, **29,** 233 (1991).

37. Fliszar S., *Charge Distributions and Chemical Effects,* Springer, New York (1983).

38. Mansour Ahmed M., Abdel Ghani Nour T., Hydrogen-bond effect, spectroscopic and molecular structure investigation of sulfamethazine Schiff-base: Experimental and quantum chemical calculations, *Journal of Molecular Structure* **1040,** 226–237 (2013).

39. Fang Zhang, Yu Zhang, Haiwei Ni, Kuirong Ma, Rongqing Li, *Spectrochimica Acta Part A: Molecular and Biomolecular Spectroscopy* **118,** 162–171 (2014).

40. Munshi P., Guru Row T.N., Intra- and intermolecular interactions in small bioactive molecules: cooperative features from experimental and theoretical charge-density analysis, *Acta Crystallogr.* **B62** 612–626 (2006).

41. Zayed Ehab M., Zayed M.A., El-Desawy M., Preparation and structure investigation of novel Schiff bases using spectroscopic, thermal analyses and molecular orbital calculations and studying their biological activities, *Spectrochimica Acta Part A: Molecular and Biomolecular Spectroscopy* **134,** 155–164 (2015).

التحليل الطيفي لمشتقات حمض المالينيلك ومقارنتها بالتحليل الحراري والحسابات النظرية والنشاط البيولوجى لها

محمد عبد الجواد زايد[١] ومحمد الدساوى[٢] وعزة عوض العدلى[٣]
[١]قسم الكيمياء – كلية العلوم – جامعة القاهرة – شارع الجامعة – الرقم البريدى21621 الجيزة - مصر.
[٢]هيئة الطاقة الذرية – قسم الفيزياء النووية- الرقم البريدي ١٣٧٥٩ - القاهرة - مصر.
[٣]مركز التميز العلمي والتكنولوجي- وزارة الأنتاج الحربي - مدينة السلام – القاهرة - مصر.

تناول هذا البحث تحضير بعض مشتقات حمض المالينيلك. وقد تم التحضير على أساس تفاعل المالنيلك أنهيدريد ومشتقات الأنيلين فى درجة حرارة الغرفة. ومعرفة التركيب الكيميائى لهم عن طريق تطبيق الطرق التحليلية المختلفة و التى شملت التحليل الميكروئى لعناصر (الكربون, الهيدروجين, النيتروجين, الاكسجين) FT-IR، وأشعة أكس، قياسات التحليلات الحرارية (TGA / DTG و DTA) بالمقارنة نظريا. كما تم الحصول على النتائج المرتبطة بالبيانات النظرية ل MOCs بواسطة طريقة DFT-B3LYP و HF 6-311++G(d,p)؛ 6-311G(d)على التوالي لتأكيد التركيب المقترح للمشتقات والتي اشارت إلى وجود علاقة كبيرة بين التقنيات النظرية والعملية. كما تم دراسة النشاط البيولوجى للمشتقات المحضرة مع الخلايا السرطانية. وأظهرت تلك المواد نشاطًا بيولوجيًا عاليًا ضد أنواع مختلفة للخلايا السرطانية مثل الخلايا السرطانية الكبدي> خلايا سرطان الثدي> خلايا سرطان القولون. التي أمكن قمعها بواسطةp-MMA > p-MOMA